

# The open pore conformation of potassium channels

Youxing Jiang, Alice Lee, Jiayun Chen, Martine Cadene, Brian T. Chait & Roderick MacKinnon

Howard Hughes Medical Institute, Laboratory of Molecular Neurobiology and Biophysics and Laboratory of Mass Spectrometry and Gaseous Ion Chemistry, Rockefeller University, 1230 York Avenue, New York, New York 10021, USA

**Living cells regulate the activity of their ion channels through a process known as gating. To open the pore, protein conformational changes must occur within a channel's membrane-spanning ion pathway. KcsA and MthK, closed and opened K<sup>+</sup> channels, respectively, reveal how such gating transitions occur. Pore-lining 'inner' helices contain a 'gating hinge' that bends by approximately 30°. In a straight conformation four inner helices form a bundle, closing the pore near its intracellular surface. In a bent configuration the inner helices splay open creating a wide (12 Å) entryway. Amino-acid sequence conservation suggests a common structural basis for gating in a wide range of K<sup>+</sup> channels, both ligand- and voltage-gated. The open conformation favours high conduction by compressing the membrane field to the selectivity filter, and also permits large organic cations and inactivation peptides to enter the pore from the intracellular solution.**

Potassium and other ion channels are allosteric proteins that switch between closed and opened conformations in response to an external stimulus in a process known as gating. Depending on the channel type, the gating stimulus can be the binding of a ligand, the membrane electric field, or both. A central issue in ion channel biophysics concerns the nature of the pore conformational changes that accompany channel gating. What do the opened and closed structures of the pore look like? In general, little is known about protein conformational changes in membrane proteins, and yet for ion channels these changes are crucial to every aspect of their function: ion conduction, gating and pharmacology. Here, we address the following questions regarding these three areas of ion channel function. For the conduction mechanism of K<sup>+</sup> channels, when the pore opens, how wide does it become, how does opening change the electric field across the pore, and how accessible is the K<sup>+</sup> selectivity filter to the intracellular solution? For the gating mechanism, what are the mechanics of pore opening, are the conformational changes within the membrane large or small? Finally, for K<sup>+</sup> channel pharmacology, which protein surfaces become exposed when the pore opens, and how might pharmacological agents interact with the closed versus opened state of the channel?

Mutational experiments from numerous laboratories have placed important structural constraints on K<sup>+</sup> channel gating. In particular, mutational studies of the Shaker voltage-dependent K<sup>+</sup> channel<sup>1,2</sup>—interpreted in the context of the KcsA K<sup>+</sup> channel structure<sup>3</sup>—identified what is probably the pore's gate. In the KcsA structure four  $\alpha$ -helices (inner helices) line the pore's intracellular half, forming a right-handed bundle (inner helix bundle) near the intracellular opening (Fig. 1)<sup>3,4</sup>. The inner helix bundle marks the point at which the Shaker pore becomes inaccessible to thiol-reactive compounds and metal ions applied to the cytoplasmic side of the channel when the channel is closed<sup>4,5</sup>. Thus, it would seem that the extracellular half of the pore, where the selectivity filter is located, is dedicated to the function of K<sup>+</sup> selectivity, and that the intracellular half, where the pore is lined by inner helices, is dedicated to gating.

In the KcsA structure the pore is very wide (about 12 Å diameter) at the centre of the membrane in what is called the central cavity, but closer to the intracellular opening, at the level of the inner helix bundle, the pore diameter narrows to about 4.0 Å (the separation between van der Waals surfaces of protein atoms) (Fig. 1). At this narrow segment, hydrophobic side chains from the inner helices line the pore, creating what would seem to be an inhospitable environ-

ment for a K<sup>+</sup> ion. Is the gate closed in the KcsA crystal structure? Functional measurements offer the best insight into the probable conformational state. In membranes, the KcsA K<sup>+</sup> channel has a very low open probability even under the acidic pH conditions known to open the channel<sup>6,7</sup>. When the intracellular carboxy-terminal 35 amino acids are truncated from KcsA, the open probability is even lower, remaining effectively near zero (C. Miller, personal communication). The crystal structures (Fig. 1) are of the truncated KcsA K<sup>+</sup> channel<sup>3,4</sup>; if structure matches function, then the truncated KcsA K<sup>+</sup> channel has a closed gate.

Exactly how do the inner helices move to open the pore? This has been a difficult question to answer in the absence of direct measurements of closed and opened channel structures. One attempt, using electron paramagnetic resonance (EPR) with spin-labelled KcsA channels, suggested that the inner helices rotate and translate (relative to the KcsA crystal structure), causing a very subtle diameter increase at the inner helix bundle (Protein Data

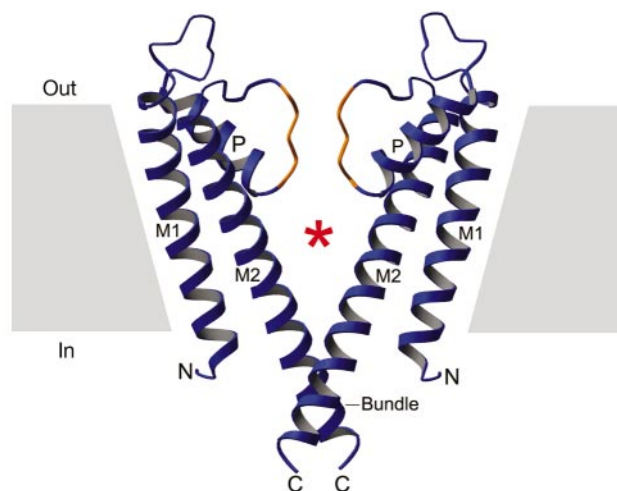


**Figure 1** Structural elements of the K<sup>+</sup> channel pore. Two subunits of the KcsA K<sup>+</sup> channel are shown with the extracellular side on top. The selectivity filter is orange and the central cavity is marked by a red asterisk. Three helical segments include, from N to C terminus, the outer helix (M1), pore helix (P) and inner helix (M2). The gate is formed by the inner helix bundle (Bundle). The figure was prepared using RIBBONS<sup>28</sup>.

Bank code 1JQ1)<sup>8,9</sup>. However, a different approach using X-ray crystallography implied that the pore might open to a much wider diameter<sup>10</sup>. The crystallographic study showed that the K<sup>+</sup> channel blocker tetrabutylammonium ion (TBA) binds in the central cavity. In the structure the inner helices remained in their apparently closed conformation, but they must have opened very wide to allow TBA (diameter 10–12 Å) to enter.

**Mechanics of pore gating**

The MthK channel from *Methanobacterium thermoautotrophicum* together with the KcsA channel provides valuable insight into the conformational changes that apparently underlie K<sup>+</sup> channel gating. The MthK channel structure includes its gating machinery (the gating ring) and contains a bound ligand (a Ca<sup>2+</sup> ion) that opens the channel in membranes<sup>11</sup> (PDB code 1LNQ). Figure 2 shows the pore structure of the MthK channel alongside the KcsA K<sup>+</sup> channel (PDB code 1K4C). Comparison between these two structures revealed first that the structure surrounding the selectivity filter is quite similar in both channels, aside from differences in the length of the extracellular ‘turret’ loops. Second, there are very large structural differences involving the inner helices: in KcsA the inner helices are nearly straight and form a bundle near the

intracellular solution, whereas in MthK the inner helices are bent and splayed open (Fig. 2a–c). Third, the bend (approximately 30°) in the MthK inner helices occurs at a hinge point—a gating hinge—that is located deep within the membrane, just below the selectivity filter. The gating hinge corresponds to Gly 83 in MthK and Gly 99 in KcsA (Fig. 3). Glycine is unique in its ability to adopt a wide range of main-chain dihedral angles and confers flexibility at specific points in protein structures. The presence of a glycine at the gating hinge permits the structural differences observed between the KcsA and MthK channels. Fourth, to convert the KcsA (closed pore) structure into the MthK (opened pore) structure, it appears as though one would simply have to exert a lateral (radial-outward) force on the C-terminal (intracellular) extent of the inner helices; such a force would place a torque on the gating hinge (Fig. 2c, d). In the open conformation the contact area between the inner and outer helices is reduced, especially near the intracellular surface. This probably accounts for the straightening of the outer helices in MthK. Finally, the open pore is very wide, about 12 Å at its narrowest point (Ala 88, Fig. 3), so that the central cavity becomes essentially continuous with the intracellular solution. The structure can be viewed in the Supplementary Information as a movie.

**Gating mechanism is conserved**

Is it reasonable to compare two different K<sup>+</sup> channels, KcsA and MthK, to infer the conformational changes that underlie gating? Structure-based sequence alignment using a wide range of K<sup>+</sup> channels suggests that it is, and that the inferred conformational changes probably occur in most K<sup>+</sup> channels (Fig. 3a). The K<sup>+</sup> channel sequences shown in Fig. 3a cover the broad range found in nature: prokaryotic, eukaryotic, channels with two and six membrane-spanning segments per subunit, ligand-gated and voltage-gated. Even cyclic nucleotide-gated (CNG) channels, which are not K<sup>+</sup> selective but are related to K<sup>+</sup> channels, apparently exhibit similar conformational changes<sup>12</sup>. The principal observation in the sequence alignment is strong amino-acid conservation at two positions in the inner helix (Fig. 3a, b). The first position is the gating hinge, conserved as glycine (red in Fig. 3a); apparently all of these channels have a gating hinge. The second position is five amino acids C-terminal to the gating hinge, conserved as alanine or glycine (green). The significance of having an amino acid with a small side chain at this second position is evident on inspection of the MthK channel structure: this amino acid points its side chain towards the pore, a large side chain would tend to plug the pore and interfere with ion conduction. Thus, the MthK structure reveals the significance of a glycine residue, to allow a flexible gating hinge, and an alanine residue, to ensure a wide pathway for ions to reach the selectivity filter. Conservation of these residues implies a conserved pore conformational change. For this reason we propose that KcsA and MthK structures represent the closed and opened states of most K<sup>+</sup> channels, ligand- and voltage-gated, as well as CNG channels.

The mechanics of pore opening may be conserved in different K<sup>+</sup> channels, but very different structures, such as integral membrane voltage sensors<sup>13,14</sup> and intracellular ligand-binding domains<sup>15</sup>, have to mechanically adapt to the pore so that they can exert a lateral force on the inner helices. Thus, the C-terminal end of the inner helices must vary in structure from one channel to the next, depending on its associated gating domain. In the MthK channel we are unable to fully resolve the connection between the pore and its gating domain, but the inner helix points at its attachment site as if the connection is nearly straight<sup>11</sup>. When the pore closes, in order for the inner helices to form a bundle—similar to the structure observed in KcsA (Fig. 2)—the connection would have to develop a bend. In this regard, much work has focused on the Pro-Val-Pro sequence near the inner helix bundle in certain voltage-dependent K<sup>+</sup> channels<sup>1</sup>. The suggestion that this sequence might make a bend seems reasonable, as a bend would direct the bottom of the inner helix towards the voltage sensor domain.

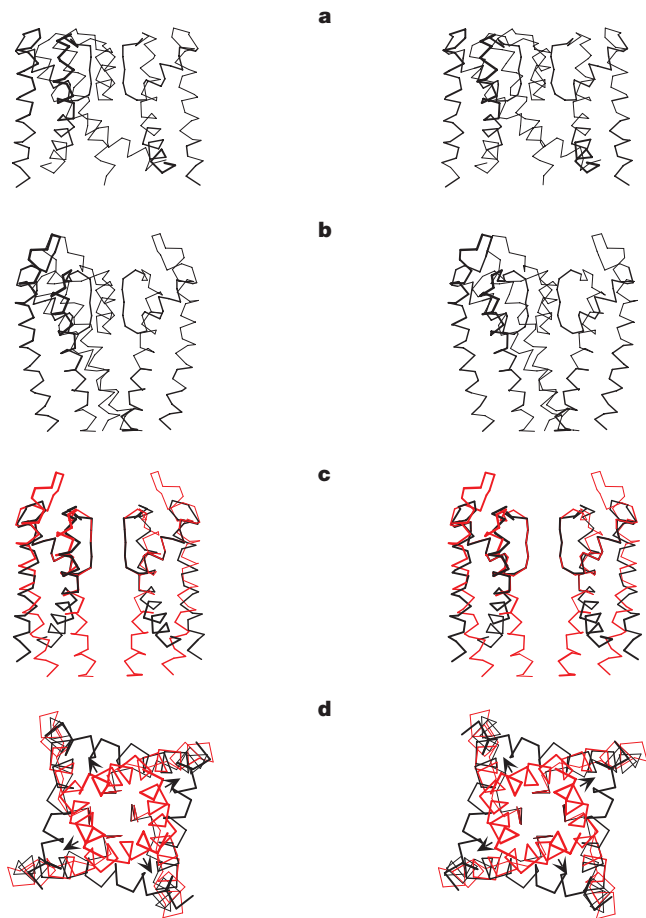


**Figure 2** Opened and closed states of K<sup>+</sup> channels. Stereo diagrams show the pore (C $\alpha$  traces) of two K<sup>+</sup> channels viewed from within the membrane: **a**, MthK (PDB code 1LNQ) (residues 19–98) and **b**, KcsA (PDB code 1K4C) (residues 24–114), with one subunit removed and oriented with the extracellular surface on top. **c**, **d**, The KcsA (red) and MthK (black) pores are superimposed and viewed from within the membrane (**c**, two subunits), and from the intracellular solution (**d**, four subunits). Only the selectivity filter and inner helices are shown in **d**. Arrows indicate the direction of inner helix displacement in going from closed (KcsA) to opened (MthK). The figures were prepared using Bobscrip<sup>29</sup>.

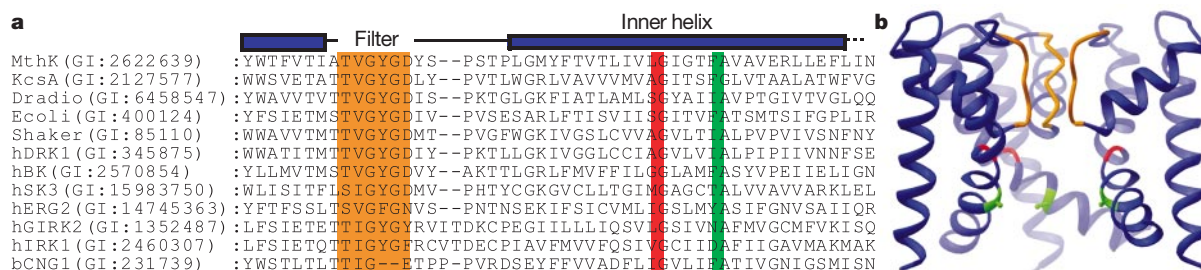


**Figure 3** Structure-based sequence analysis suggests conserved gating conformations. **a**, Sequences from the inner helices of various K<sup>+</sup> channels and a CNG channel. The selectivity filter is coloured orange, the gating hinge glycine red, and the amino acid at the narrowest point of the MthK intracellular pore entryway, green. MthK, *M. thermautotrophicum* K<sup>+</sup> channel; KcsA, *Streptomyces lividans* K<sup>+</sup> channel; Dradio, *Deinococcus radiodurans* K<sup>+</sup> channel; Ecoli, *Escherichia coli* K<sup>+</sup> channel; Shaker,

*Drosophila melanogaster* K<sup>+</sup> channel; hDRK1, *Homo sapiens* K<sup>+</sup> channel; hBK, *H. sapiens* BK channel; hSK3, *H. sapiens* SK channel; hERG2, *H. sapiens* K<sup>+</sup> channel; hGIRK2, *H. sapiens* G-protein-activated K<sup>+</sup> channel 2; hIRK1, *H. sapiens* K<sup>+</sup> channel; bCNG1, *Bos taurus* cyclic nucleotide-gated channel. Protein ID numbers are indicated in parentheses. **b**, Three subunits of the MthK pore with colours corresponding to **a**.

### Pharmacology and inactivation gating

The wide diameter of the open gate (12 Å) is entirely consistent with the experiments of Armstrong, showing that large organic cations block the intracellular entryway of K<sup>+</sup> channels<sup>16,17</sup> (Fig. 4). The open gate is wide enough so that organic compounds can enter from the cytoplasm and reach the membrane centre (the cavity) before lodging just beneath the selectivity filter<sup>10</sup>. It is interesting to see that gate closure (the pinching shut of the inner helix bundle) occurs while maintaining the size of the cavity (Fig. 2). This structural feature of K<sup>+</sup> channel gating is consistent with the phenomenon of functional ‘trapping’ of organic cations behind the gate, deep within the pore<sup>16–18</sup>. The structure of the open pore builds on our understanding of the susceptibility of K<sup>+</sup> channels to block by organic cations, including many commonly prescribed pharmacological agents<sup>19</sup>. On the intracellular side of the selectivity filter the pore is hydrophobic<sup>3</sup>, cation attractive (owing to oriented pore helices)<sup>20</sup> and wide (Fig. 4). These properties of K<sup>+</sup> channels undoubtedly lie at the basis of certain drug-induced cardiac conduction abnormalities such as acquired long-QT syndrome<sup>19</sup>.

The structure of the open pore helps us to further understand a form of K<sup>+</sup> channel gating known as inactivation. A-type K<sup>+</sup> channels such as the Shaker K<sup>+</sup> channel open in response to membrane depolarization, but a few milliseconds later they stop

conducting ions because an inactivation gate blocks the pore on the intracellular side<sup>21,22</sup>. A ‘ball and chain’ mechanism was proposed about thirty years ago for a similar process in Na<sup>+</sup> channels<sup>23,24</sup>. Ten years ago, the ‘ball and chain’ inactivation gate of A-type K<sup>+</sup> channels was shown to be formed by the channel’s own amino terminus<sup>21,22</sup>, or the N terminus of an associated β-subunit<sup>25</sup>. Recently, on the basis of a mutational study, it was proposed that an N-terminal inactivation gate blocks ion conduction by entering into the pore as an extended peptide, reaching to the cavity<sup>10</sup>. The mutational data were convincing, but nevertheless, given the narrow

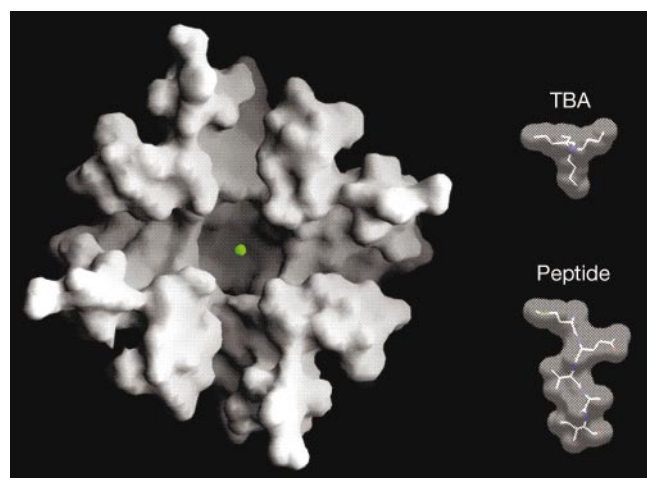


**Figure 4** The open pore allows entry of large molecules from the intracellular solution. Molecular surface of the MthK pore (all side chains included) viewed from the intracellular solution. A K<sup>+</sup> ion in the selectivity filter is shown as a green sphere. Surface models of tetrabutylammonium (TBA) and the N-terminal inactivation gate (sequence MQVS) from KvB1.1 (peptide) are shown<sup>10</sup>. The figure was prepared using GRASP<sup>20</sup>.

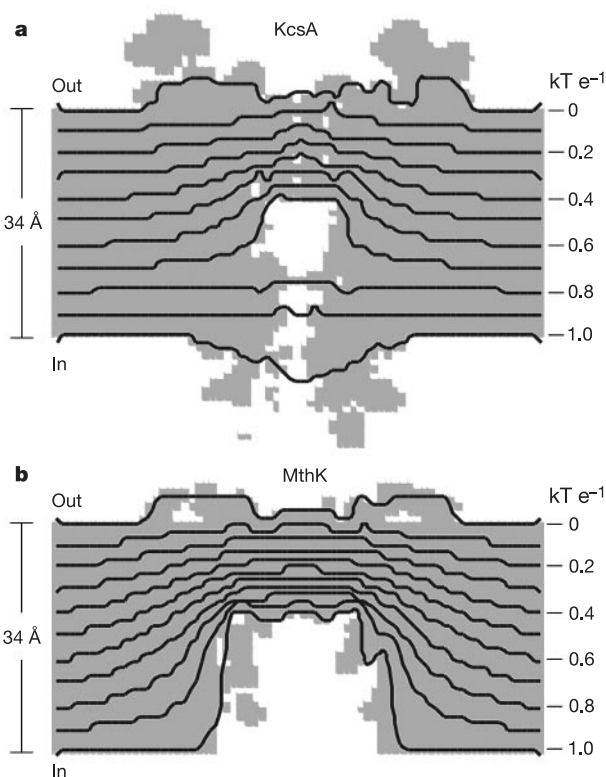


**Figure 5** The membrane electric potential across the pore changes on opening. **a**, **b**, Electrostatic contour plots for KcsA (**a**) and MthK (**b**) in a membrane. Electric potential was calculated as described (see Methods). A slice perpendicular to the membrane through the channel shows the pore between the intracellular solution (bottom) and extracellular solution (top). The grey region corresponds to protein or membrane (dielectric constant 2); white regions to aqueous solution (dielectric constant 80). Potential runs from 1.0 to 0 with contours every 0.1 kT e<sup>-1</sup>.

inner pore of KcsA the proposal seemed unbelievable from a structural perspective. The open channel structure of MthK, however, gives a different impression, and rationalizes the mutational results (Fig. 4). The open pore is wide enough so that an extended peptide can insert its N terminus (cationic) into the cavity.

**Membrane potential across the open pore**

The open pore conformation has important implications for ion conduction, in part because the electric field experienced by an ion in the pore depends on the shape of the pore, among other factors. To gain a qualitative appreciation for the effect of pore shape, we calculated the electrostatic potential for the KcsA and MthK pores, closed and opened K<sup>+</sup> channels, embedded in a membrane by solving the finite difference Poisson equation. The dielectric constant for the protein and membrane were set at 2.0, and for water outside the membrane and in the pore, 80. To focus on the effect of pore shape on applied membrane potential the protein was uncharged. The results are shown in the form of electrostatic contour plots (Fig. 5). In the open conformation the cavity is at the same membrane potential as the internal solution. This Poisson calculation gives the potential under equilibrium, when ions are not moving through the pore. The qualitative result is impressive: an open K<sup>+</sup> channel effectively thins the membrane for a diffusing K<sup>+</sup> ion to approximately the 12 Å length of the selectivity filter. That is, the access resistance for a K<sup>+</sup> ion diffusing between the cytoplasm and the selectivity filter is low. This feature of K<sup>+</sup> channels undoubtedly contributes to their high conductance.

**Discussion**

On the basis of the opened MthK channel, the closed KcsA channel, and amino-acid sequence analysis, we propose a structural basis for gating transitions in the transmembrane pore of K<sup>+</sup> channels. The four inner helices can exist in a straight (apparently relaxed) conformation in which case they form a bundle that closes the pore near its intracellular opening. Alternatively the inner helices can bend, causing the bundle to splay open to a diameter of about 12 Å. The principal structural feature of the gating conformational change is the presence of a gating hinge located deep within the membrane, conserved as a glycine residue in most K<sup>+</sup> channels. The gating conformational changes within the membrane are very large, but are mainly confined to the intracellular half of the channel. Based on amino-acid sequence conservation, we propose that different K<sup>+</sup> channels, ligand- and voltage-gated, as well as cyclic nucleotide-gated channels, undergo similar pore conformational changes. □

**Methods**

**Electrostatic calculation**

Electrostatic potential was calculated by solving the finite difference Poisson equation using a program written in Fortran 77 implementing a Jacobi relaxation algorithm<sup>26,27</sup>. The KcsA and MthK pores were mapped onto a 70 × 70 × 90 Å cubic grid with spacings of 1.0 Å. Side chains were added to the MthK pore structure for defining the region of space bounded by the channel. Channels were placed into a 34 Å thick slab of dielectric constant 2.0 used to model the membrane. The protein region was assigned a dielectric constant of 2.0 using the standard Pauling atomic radii; if an atom intersected a grid element then a dielectric constant of 2.0 was assigned to the element. We did not use protein charges in the calculation. Solution surrounding the membrane and in the pore was assigned a dielectric constant of 80. Ionic strength outside the membrane had only a small effect on the potential within the membrane and therefore was kept at 0 for producing Fig. 5.

Received 22 March; accepted 22 April 2002.

1. del Camino, D., Holmgren, M., Liu, Y. & Yellen, G. Blocker protection in the pore of a voltage-gated K<sup>+</sup> channel and its structural implications. *Nature* **403**, 321–325 (2000).  
 2. Liu, Y., Holmgren, M., Jurman, M. E. & Yellen, G. Gated access to the pore of a voltage-dependent K<sup>+</sup> channel. *Neuron* **19**, 175–184 (1997).

3. Doyle, D. A. *et al.* The structure of the potassium channel: molecular basis of K<sup>+</sup> conduction and selectivity. *Science* **280**, 69–77 (1998).  
 4. Zhou, Y., Morais-Cabral, J. H., Kaufman, A. & MacKinnon, R. Chemistry of ion coordination and hydration revealed by a K<sup>+</sup> channel–Fab complex at 2.0 Å resolution. *Nature* **414**, 43–48 (2001).  
 5. del Camino, D. & Yellen, G. Tight steric closure at the intracellular activation gate of a voltage-gated K<sup>+</sup> channel. *Neuron* **32**, 649–656 (2001).  
 6. Cuello, L. G., Romero, J. G., Cortes, D. M. & Perozo, E. pH-dependent gating in the *Streptomyces lividans* K<sup>+</sup> channel. *Biochemistry* **37**, 3229–3236 (1998).  
 7. Heginbotham, L., LeMasurier, M., Kolmakova-Partensky, L. & Miller, C. Single streptomyces lividans K<sup>+</sup> channels. Functional asymmetries and sidedness of proton activation. *J. Gen. Physiol.* **114**, 551–560 (1999).  
 8. Perozo, E., Cortes, D. M. & Cuello, L. G. Structural rearrangements underlying K<sup>+</sup>-channel activation gating. *Science* **285**, 73–78 (1999).  
 9. Liu, Y. S., Sompornpisut, P. & Perozo, E. Structure of the KcsA channel intracellular gate in the open state. *Nature Struct. Biol.* **8**, 883–887 (2001).  
 10. Zhou, M., Morais-Cabral, J. H., Mann, S. & MacKinnon, R. Potassium channel receptor site for the inactivation gate and quaternary amine inhibitors. *Nature* **411**, 657–661 (2001).  
 11. Jiang, Y. *et al.* Crystal structure and mechanism of a calcium-gated potassium channel. *Nature* **417**, 515–522 (2002).  
 12. Flynn, G. E., Johnson, J. P. Jr & Zagotta, W. N. Cyclic nucleotide-gated channels: shedding light on the opening of a channel pore. *Nature Rev. Neurosci.* **2**, 643–651 (2001).  
 13. Sigworth, F. J. Voltage gating of ion channels. *Q. Rev. Biophys.* **27**, 1–40 (1994).  
 14. Bezanilla, F. The voltage sensor in voltage-dependent ion channels. *Physiol. Rev.* **80**, 555–592 (2000).  
 15. Jiang, Y., Pico, A., Cadene, M., Chait, B. T. & MacKinnon, R. Structure of the RCK domain from the *E. coli* K<sup>+</sup> channel and demonstration of its presence in the human BK channel. *Neuron* **29**, 593–601 (2001).  
 16. Armstrong, C. M. Interaction of tetraethylammonium ion derivatives with the potassium channels of giant axons. *J. Gen. Physiol.* **58**, 413–437 (1971).  
 17. Armstrong, C. M. Ionic pores, gates, and gating currents. *Q. Rev. Biophys.* **7**, 179–210 (1974).  
 18. Holmgren, M., Smith, P. L. & Yellen, G. Trapping of organic blockers by closing of voltage-dependent K<sup>+</sup> channels: evidence for a trap door mechanism of activation gating. *J. Gen. Physiol.* **109**, 527–535 (1997).  
 19. Mitcheson, J. S., Chen, J., Lin, M., Culbertson, C. & Sanguinetti, M. C. A structural basis for drug-induced long QT syndrome. *Proc. Natl. Acad. Sci. USA* **97**, 12329–12333 (2000).  
 20. Roux, B. & MacKinnon, R. The cavity and pore helices in the KcsA K<sup>+</sup> channel: electrostatic stabilization of monovalent cations. *Science* **285**, 100–102 (1999).  
 21. Hoshi, T., Zagotta, W. N. & Aldrich, R. W. Biophysical and molecular mechanisms of Shaker potassium channel inactivation. *Science* **250**, 533–538 (1990).  
 22. Zagotta, W. N., Hoshi, T. & Aldrich, R. W. Restoration of inactivation in mutants of Shaker potassium channels by a peptide derived from ShB. *Science* **250**, 568–571 (1990).  
 23. Bezanilla, F. & Armstrong, C. M. Inactivation of the sodium channel. I. Sodium current experiments. *J. Gen. Physiol.* **70**, 549–566 (1977).  
 24. Armstrong, C. M. & Bezanilla, F. Inactivation of the sodium channel. II. Gating current experiments. *J. Gen. Physiol.* **70**, 567–590 (1977).  
 25. Rettig, J. *et al.* Inactivation properties of voltage-gated K<sup>+</sup> channels altered by presence of β-subunit. *Nature* **369**, 289–294 (1994).  
 26. Warwicker, J. & Watson, H. C. Calculation of the electric potential in the active site cleft due to alpha-helix dipoles. *J. Mol. Biol.* **157**, 671–679 (1982).  
 27. Klapper, I., Hagstrom, R., Fine, R., Sharp, K. & Honig, B. Focusing of electric fields in the active site of Cu-Zn superoxide dismutase: effects of ionic strength and amino-acid modification. *Proteins* **1**, 47–59 (1986).  
 28. Carson, M. Ribbons. *Methods Enzymol.* **277**, 493–505 (1997).  
 29. Esnouf, R. M. An extensively modified version of MolScript that includes greatly enhanced coloring capabilities. *J. Mol. Graph. Model.* **15**, 132–133 (1997).  
 30. Nicholls, A., Sharp, K. A. & Honig, B. Protein folding and association: insights from the interfacial and thermodynamic properties of hydrocarbons. *Proteins* **11**, 281–296 (1991).

Supplementary Information accompanies the paper on Nature’s website (<http://www.nature.com>).

**Acknowledgements**

We thank the staff at the National Synchrotron Light Source, Brookhaven National Laboratory, X-25, the Cornell High Energy Synchrotron Source, F1, and the Advanced Light Source, Lawrence Berkeley Laboratory, 5.0.2 for synchrotron support; members of the MacKinnon laboratory for assistance; R. Dutzler and R. Xie for programming and graphical assistance; F. Sigworth, P. Jordan, C. Miller and D. Gadsby for discussions; and W. Chin for help in manuscript preparation. This work was supported by grants from the NIH to R.M. and from the National Center for Research Resources, NIH, to B.T.C. R.M. is an investigator in the Howard Hughes Medical Institute.

**Competing interests statement**

The authors declare that they have no competing financial interests.

Correspondence and requests for materials should be addressed to R.M. (e-mail: mackinn@rockvax.rockefeller.edu). Coordinates have been deposited with the Protein Data Bank under accession code 1LNQ.